EFFICIENT SIDELOBE REDUCTION TECHNIQUE FOR SMALL-SIZED CONCENTRIC CIRCULAR ARRAYS

M. Dessouky, H. Sharshar, and Y. Albagory

Department of Electronics
and Electrical Communications Engineering
Faculty of Electronic Engineering
Menouf, Egypt

Abstract—Concentric circular antenna array (CCAA) has interesting features over other array configurations. A uniform arrangement of elements is assumed where the interelement spacing is kept almost half of the wavelength and the array parameters such as the steering matrix and gain are determined. The array performance such as beam power pattern, sidelobe level and beamwidth are discussed in two cases of central element feeding. The two cases are compared showing the reduction in the sidelobe level to more than 20 dB in the case of central element feeding without extra signal processing especially for small-sized arrays that have smaller number of elements and rings.

1. INTRODUCTION

Antenna arrays have been used widely in different applications including radar [1], sonar [2], biomedicine [3], communications [4], and imaging [5]. Antenna arrays may be linear, two-dimensional, circular and spherical in element arrangement. A very popular type of antenna arrays is the circular array which has several advantages over other schemes such as all-azimuth scan capability (i.e., it can perform 360 scan around its center) and the beam pattern can be kept invariant. Concentric circular antenna array (CCAA) that contains many concentric circular rings of different radii and number of elements have several advantages including the flexibility in array pattern synthesis and design both in narrowband and broadband beamforming applications [6–12]. CCAA is also favored in direction of arrival (DOA) applications since it provides almost invariant azimuth angle coverage. In this paper we study mostly uniform CCAA that have a halfwave element separation both between the individual arrays

and the interelement spacing in the same array. The beam pattern, sidelobe level and beamwidth are examined for two cases; the first with no central element feeding and the other with the existence of such element. It is found that the existence of the central element can control the sidelobe level with minimal beamwidth increase. The paper is arranged as follows; in Section 2, the array geometry and its array steering matrix is defined for beamforming applications. Section 3 studies the almost halfwave UCCAA while Section 4 determines the variations of beam pattern, sidelobe level and beamwidth. In Section 5, the performance of the array is discussed for the case of central element feeding and finally Section 6 concludes the paper.

2. GEOMETRY AND ARRAY STEERING MATRIX OF UCCAA

The arrangement of elements in such arrays may contain multiple concentric circular rings which differ in radius and number of elements and this gives arise to different radiation patterns. Figure 1 shows the configuration of concentric circular arrays in which there are M concentric circular rings. The mth ring has a radius r_m and number of elements N_m where $m = 1, 2, \ldots, M$. Assuming that the elements
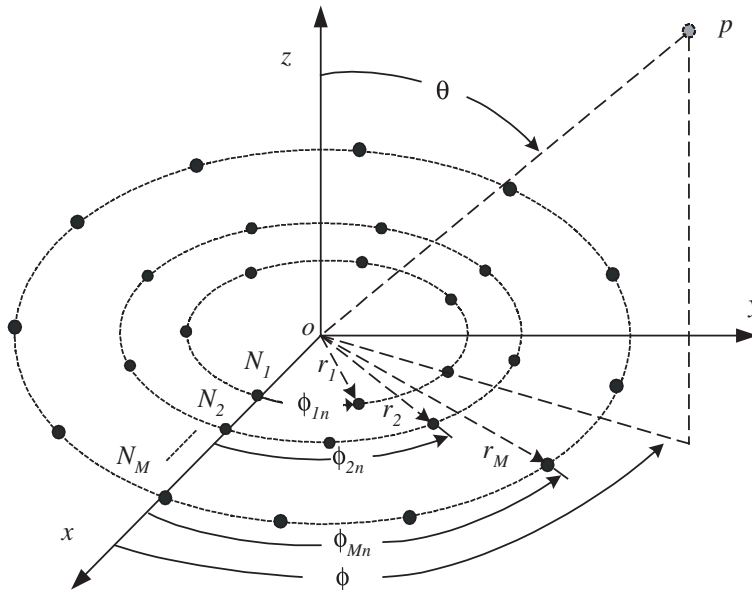

Figure 1. Concentric circular antenna arrays (CCAA).

are uniformly spaced within the ring so it has an element angular separation given by

$$\psi_m = \frac{2\pi}{N_m} \tag{1}$$

and the elements in this ring are therefore located with an angle measured from the x-axis given by

$$\phi_{mn} = n\psi_m, \qquad n = 1, 2, \ldots, N_m \tag{2}$$

The field measured at the observation point P is given by

$$E_m(r, \theta, \phi) = \frac{e^{-jkr}}{r} \sum_{n=1}^{N_m} \alpha_{mn} e^{jkr_m \sin\theta \cos(\phi - \phi_{mn})} \tag{3}$$

where $k = \frac{2\pi}{\lambda}$ is the wave number and α_{mn} is the excitation coefficients (amplitude and phase) of the mn^{th} element. An expression for the array steering matrix can be deduced by first defining the array steering vector for a single ring and extending the analysis for the whole array. For the mth ring, the array steering vector has elements given by

$$s_{mn}(\theta, \phi) = e^{jkr_m \sin\theta \cos(\phi - \phi_{mn})} \qquad n = 1, 2, \ldots, N_m \tag{4}$$

therefore the array steering vector for such ring will be:

$$S_m(\theta, \phi) = \left[e^{jkr_m \sin\theta \cos(\phi - \phi_{m1})} e^{jkr_m \sin\theta \cos(\phi - \phi_{m2})} \ldots \right.$$
$$\left. e^{jkr_m \sin\theta \cos(\phi - \phi_{mn})} \ldots e^{jkr_m \sin\theta \cos(\phi - \phi_{mN_m})} \right]^T \tag{5}$$

Now, the array steering matrix can be formulated as:

$$AS(\theta, \phi) = [S_1(\theta, \phi) S_2(\theta, \phi) \ldots \ldots S_m(\theta, \phi) \ldots \ldots S_M(\theta, \phi)] \tag{6}$$

Generally, the rings may have different number of elements and the array steering vectors of the rings have unequal lengths, therefore we append lower dimension vectors with zeros. In most cases the maximum number of elements will be the outermost ring, where it has N_M elements and therefore it will determine the steering matrix size which in this case is $N_M \times M$. For this case the array steering matrix will be

$AS(\theta, \phi) =$

$$
\begin{bmatrix}
e^{jkr_1 \sin\theta \cos(\phi-\phi_{11})} & e^{jkr_2 \sin\theta \cos(\phi-\phi_{21})} & e^{jkr_M \sin\theta \cos(\phi-\phi_{M1})} \\
e^{jkr_1 \sin\theta \cos(\phi-\phi_{12})} & e^{jkr_2 \sin\theta \cos(\phi-\phi_{22})} & e^{jkr_M \sin\theta \cos(\phi-\phi_{M2})} \\
. & . & . \\
e^{jkr_1 \sin\theta \cos(\phi-\phi_{1N_1})} & . & . \\
0 & e^{jkr_2 \sin\theta \cos(\phi-\phi_{2N_2})} & . \\
0 & 0 & . \\
0 & 0 & e^{jkr_M \sin\theta \cos(\phi-\phi_{MN_{M-1}})} \\
0 & 0 & e^{jkr_M \sin\theta \cos(\phi-\phi_{MN_M})}
\end{bmatrix}
$$

$$(7)$$

We can control the radiation pattern of the array by controlling the magnitudes and phases of the exciting currents. Therefore the array factor or gain will be determined by the following equation

$$G(\theta, \phi) = SUM\left\{W(\theta, \phi)^H AS(\theta, \phi)\right\} \tag{8}$$

where the SUM operator is the summation of the elements of the resulted matrix and $W(\theta, \phi)$ is the weight matrix that controls the amplitudes and phases of the input currents. To have a delay-and-sum beamformer, we form the main lobe in the direction (θ_o, ϕ_o) by equaling the weight matrix by the array steering matrix at the same direction or

$$W(\theta, \phi) = AS(\theta_o, \phi_o) \tag{9}$$

and therefore, the normalized array gain is given by

$$G_n(\theta, \phi) = \frac{1}{\sum\limits_{i=1}^{M} N_i} SUM\left\{AS(\theta_o, \phi_o)^H \, AS(\theta, \phi)\right\} \tag{10}$$

3. $\lambda/2$ ELEMENT-SPACING UCCAA

Each the number of elements in each ring, the interelement spacing and the inter-ring spacing will affect the array performance such as the beamwidth and sidelobe level. We consider here the array that has almost $\lambda/2$ element-separation. Recalling the element factor given in Eq. (4) where it can be rewritten as

$$s_{mn}(\theta, \phi) = e^{jN_m a_m \sin\theta \cos(\phi-\phi_{mn})} \tag{11}$$

where

$$a_m = \frac{2\pi r_m}{N_m \lambda} \tag{12}$$

is the normalized element-arc-separation of the mth ring. The normalized ring radius is given by

$$\dot{r}_m = \frac{a_m N_m}{2\pi} \tag{13}$$

and the normalized array area will be

$$\dot{A}_m = \pi \dot{r}_M^2 \tag{14}$$

For any two successive rings, the normalized ring-radial-separation is given by

$$d_m = \dot{r}_{m+1} - \dot{r}_m \tag{15}$$

If n_i is the element increment given by

$$n_i = N_{m+1} - N_m \tag{16}$$

Assuming $a_{m+1} = a_m$, therefore we have

$$d_m = \frac{n_i a_m}{2\pi} \tag{17}$$

and the needed element increment will be

$$n_i = \frac{2\pi d_m}{a_m} \tag{18}$$

and the total number of elements in the whole CCAA will be

$$N_t = MN_1 + \sum_{k=1}^{M-1} k n_i \tag{19}$$

For $\lambda/2$ element arc-separation (i.e., element separation within the ring is one half the wavelength or $a_m = 0.5$), if the element increment is one element per ring outwardly, then the normalized ring radius will be incremented by

$$d_m = \frac{1}{4\pi} \tag{20}$$

thus the ring-radial-separation increases by a fixed value that equals 0.079577471 of the wavelength for one element increments. Figure 2 depicts the variation of the normalized ring-radial-separation versus element increment. From this figure, it can be noticed that the most
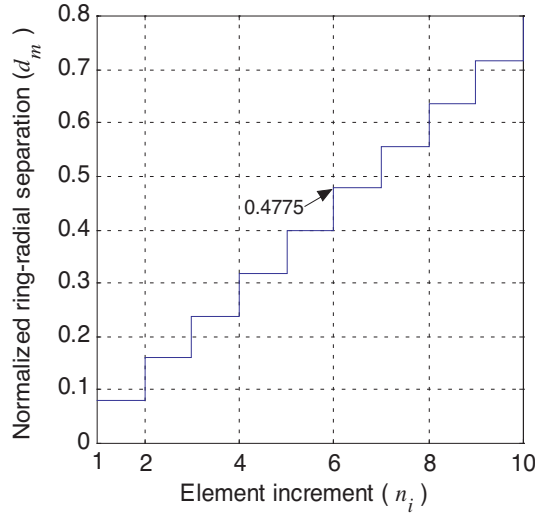
Figure 2. Normalized ring-radial-separation versus element increment.

element increments that give the nearest half wave radial separation are $n_i = 6$ and 7 at which $d_m = 0.4775$ and 0.557 respectively. The performance of CCAA is affected by the number of elements in each ring, the radial separation and the number of rings. Choosing the element increment value will affect the performance of the UCCAA such as the half power beamwidth, the 1st sidelobe level, the total number of elements in the array and the array normalized area. For a $\lambda/2$-UCCAA (i.e., the element increment $n_i = 6$ or $d_m = 0.4775$ and $a_m = 0.5$) that has an inner ring number of elements N_1, the total number of elements in the array will be

$$N_t = MN_1 + \sum_{k=1}^{M-1} 6k \qquad (21)$$

Figure 3 depicts the variation of the total number of elements with the number of rings at different values of N_1.

4. BEAM POWER PATTERN, SIDELOBE LEVELS AND BEAMWIDTH

For uniform $\lambda/2$-UCCAA, both the number of rings of the array (M) and the number of elements of the innermost circle (N_1) will affect the
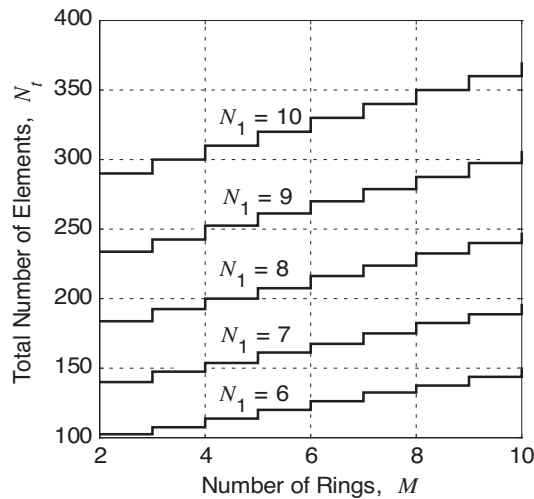
Figure 3. Total number of elements versus number of rings at different inner ring size.

array performance such as power pattern, beamwidth and sidelobe levels. We may show these variations as functions of both beam direction and the total number of elements or the array size at different values of N_1. Figures 4a and 4b depict the effect of the array geometry on the power pattern. The arrays in these figures has constant number of rings but of different number of elements for the innermost ring. It is apparent from these figures that the beamwidth will be narrower slightly with the increase of the innermost ring size and the sidelobe levels will be affected also where it can be reduced at some directions. Figures 5a and 5b shows the effect of increasing the number of rings at constant starting inner ring of 5 elements. All the curves in Figs. 4a, 4b, 5a, and 5b are drawn in three planes of ϕ (i.e., $0°, 45°, 90°$) and they all show the same variations therefore they are identical. The first sidelobe level will be affected by increasing the number of rings where it decreases and the sidelobes increase in number and gets more closer to each other. In Fig. 6, the values show the decrease of its level with increasing the array size at different values of N_1. All curves in this figure will converge to about $-17.5\,\mathrm{dB}$ level for normalized array (i.e., the mainlobe has $0\,\mathrm{dB}$ gain) when we increase the number of elements. Changing the beam direction will affect very slightly on the sidelobe level at constant other parameters and seems to be constant, while Fig. 7 shows the variation of B_θ (i.e., the beamwidth in the θ-direction) with both of the beam direction and the number of rings at
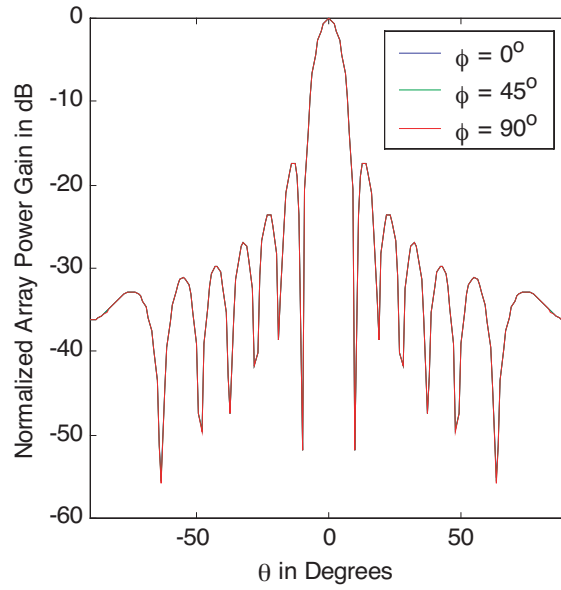
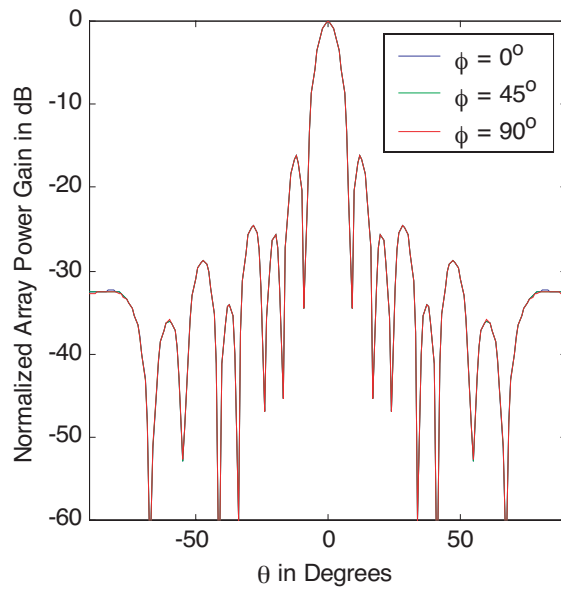**Figure 4a.** Beam power pattern for $N_1 = 5$, $M = 7$.

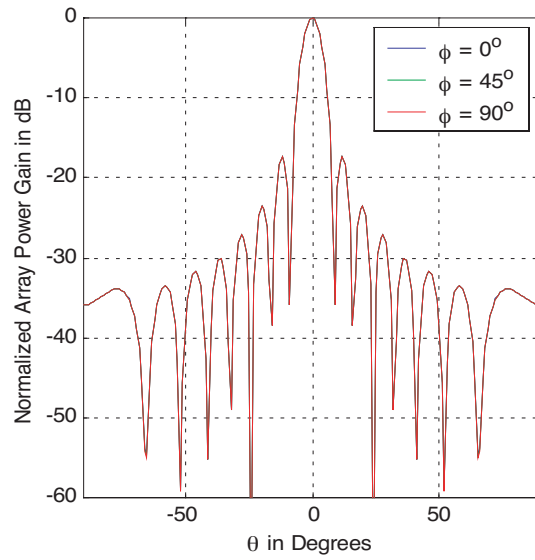
Figure 4b. Beam power pattern for $N_1 = 10$, $M = 7$.

Figure 5a. Beam power pattern for $N_1 = 5$, $M = 8$.
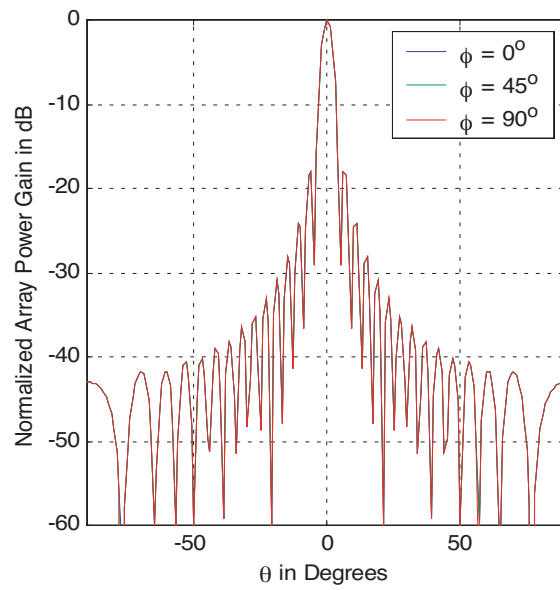

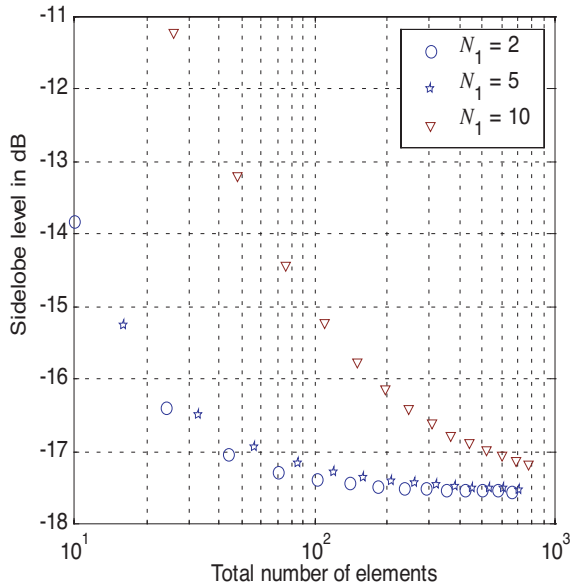**Figure 5b.** Beam power pattern for $N_1 = 5$, $M = 15$.

Figure 6. Sidelobe level versus number of array elements at different size of the innermost ring.
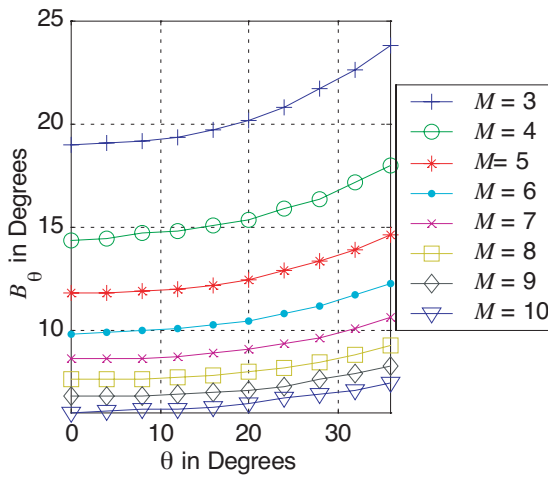

Figure 7. Beamwidth variation with beam direction at different number of rings for $N_1 = 5$ UCCAA.
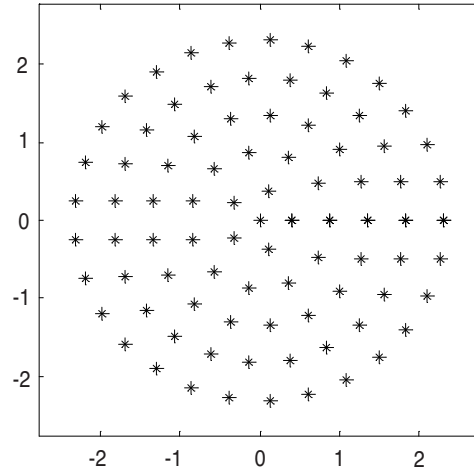
Figure 8. Center-fed UCCAA geometry for $N_1 = 5$ and $M = 5$.

different number of elements of the innermost tier. As depicted from these figures, the beamwidth increases as the beam directed away from the broadside direction of the array but decreases with increasing the number of rings and the number of elements of the innermost ring also.

5. CENTRAL ELEMENT FEEDING EFFECTS ON THE UCCAA PERFORMANCE

The UCCAA can be center fed by placing an element at the center of the array as shown for example in Fig. 8. This element will affect both the sidelobe level and beamwidth. We notice for this configuration that the sidelobe level will be reduced at the cost of some minor increase in beamwidth. Figure 9 shows the variation in beamwidth for the two cases of feeding indicating some increase in the beamwidth. The increase in beamwidth will be smaller for larger innermost ring CCAA. The element will increase the array factor by the current weighting or factor of that element or α_o, therefore we can rewrite the array gain as

$$G(\theta, \phi) = SUM \left\{ AS(\theta_o, \phi_o)^H AS(\theta, \phi) \right\} + \alpha_o \qquad (22)$$

and the normalized array gain will be

$$G_n(\theta, \phi) = \frac{1}{\alpha_o + N_t} SUM \left\{ AS(\theta_o, \phi_o)^H AS(\theta, \phi) \right\} \qquad (23)$$
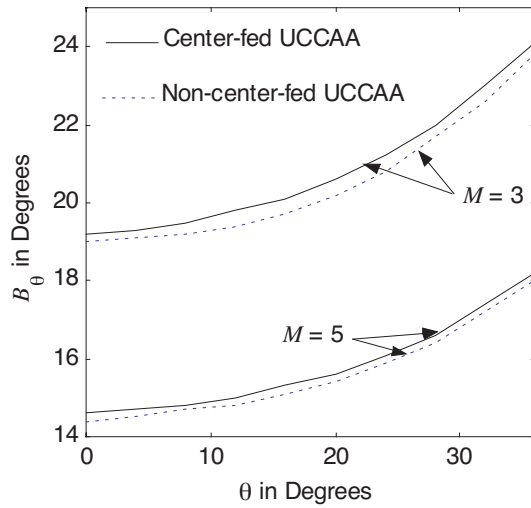
Figure 9. Beamwidth variations for the two cases of central element feeding at $M = 3$ and 5.
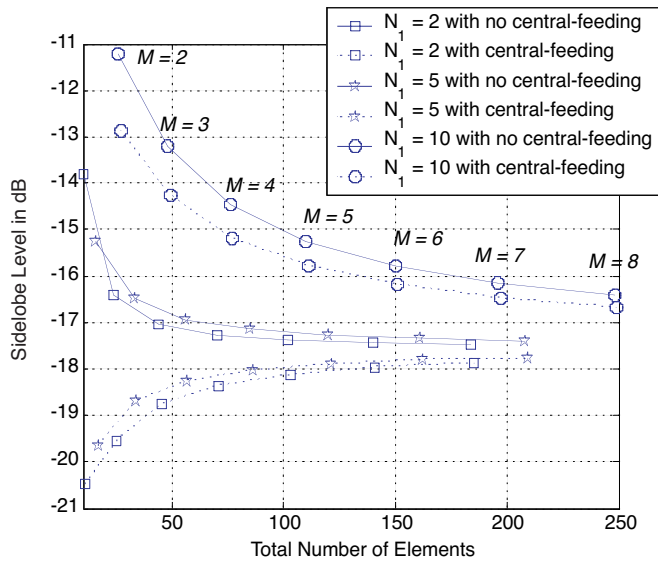

Figure 10. First sidelobe level variation in UCCAA for the two cases of central element feeding.

The added element may be considered as an innermost circular array of N_o elements but with radius tends to zero and weighted by α_o/N_o. Figure 10 demonstrates the effect of center feeding on the sidelobe levels, in which the dashed curves are for the case of center-fed arrays while the solid are for the other case. The sidelobe level decreases in the case of center feeding and the reduction will be more for smaller innermost ring CCAA. For example the 121 element center-fed array will be down by 0.62 dB than for 120 element regular array without center feeding while there is an increase in beamwidth by about 0.025 degrees only. The reduced sidelobes are obtained without extra signal processing complexity and this level may approach more than 20 dB as shown in Fig. 10.

6. CONCLUSION

Uniform concentric circular antenna arrays (UCCAA) have been discussed and the array parameters such as the array steering matrix and normalized gain are defined. The array steering matrix is useful in the beamforming applications as well as direction of arrival (DOA) estimation applications. The array beam pattern was discussed as a function of the number of element of the innermost circular array, the number of concentric arrays, and both the element separation in the individual array and inter-ring separation. The performance of UCCAA in terms of beam pattern, sidelobe level and beamwidth are discussed showing their variations with the array geometry in two cases of the central element feeding. The existence of the central element in the UCCAA may reduce the sidelobe level more than 20 dB without complicated signal processing.

REFERENCES

1. Munson, D. C., J. D. O'Brian, and W. K. Jenkins, "A tomographic formulation of spot-light mode synthetic aperture radar," *Proc. IEEE,* Vol. 71, 917–925, Aug. 1983.
2. Owsley, N. L., *Array Signal Processing,* S. Haykin (ed.), Prentice-Hall, Englewood Cliffs, NJ, 1985.
3. Peterson, P. M., N. I. Durlach, et al., "Multimicrophone adaptive beamforming for interference reduction in hearing aids," *Jour. of Rehab. R&D,* Vol. 24, Fall 1987.
4. Compton, R. T., "An adaptive array in a spread-spectrum communication system," *Proc. IEEE,* Vol. 66, 289–298, Mar. 1978.

5. Kak, A. C., *Array Signal Processing,* S. Haykin (ed.), Prentice-Hall, Englewood Cliffs, NJ, 1985.

6. Fletcher, P. and P. Darwood, "Beamforming for circular and semicircular array antennas for low-cost wireless lan data communications systems," *IEE Proc. Microwaves, Antennas and Propagation,* Vol. 145, No. 2, 153–158, Apr. 1998.

7. Bogdan, L. and C. Comsa, "Analysis of circular arrays as smart antennas for cellular networks," *Proc. IEEE Int. Symp. Signals, Circuits and Systems'03,* Vol. 2, 525–528, July 2003.

8. Chan, S. C. and C. K. S. Pun, "On the design of digital broadband beamformer for uniform circular array with frequency invariant characteristics," *Proc. IEEE ISCAS'02,* Vol. 1, I-693–I-696, Arizona, USA, May 2002.

9. Li, Y., K. C. Ho, and C. Kwan, "A novel partial adaptive broad-band beamformer using concentric ring array," *Proc. IEEE ICASSP'04,* II-177–II-180, Montreal, Quebec, Canada, May 2004.

10. Wan, J. X., J. Lei, and C.-H. Liang, "An efficient analysis of large-scale periodic microstrip antenna arrays using the characteristic basis function method," *Progress In Electromagnetics Research*, PIER 50, 61–81, 2005.

11. Mouhamadou, M., P. Armand, P. Vaudon, and M. Rammal, "Interference supression of the linear antenna arrays controlled by phase with use of SQP algorithm," *Progress In Electromagnetics Research*, PIER 59, 251–265, 2006.

12. Sanyal, S. K., Q. M. Alfred, and T. Chakravarty, "A novel beam-switching algorithm for programmable phased array antenna," *Progress In Electromagnetics Research*, PIER 60, 187–195, 2006.